CHAPTER II
BACKGROUND AND LITERATURE SURVEY

2.1 Background

2.1.1 Two-Phase Flow

For vertical pipe, there are five main regimes, shown in Figure 2.1 through Figure 2.2, occurring successively at ever-increasing gas flow rates:

(a) *Bubble flow*: There is a continuous liquid and the gas phase dispersed as bubble within the liquid continuum. The bubbles travel with complex motion causing the bubbles coalescing and generally of non-uniform size.

(b) *Slug flow*: This flow pattern, which in vertical systems is sometime referred to as plug flow, occurs when the bubble size tends toward that of the channel diameter, and characteristic bullet-shaped bubbles are formed. A bubble surrounded by liquid thin film is often called a Taylor bubble. The liquid between the Taylor bubbles often contains a dispersion of smaller bubbles.

(c) *Churn flow*: At higher gas velocities, the Taylor bubbles in slug flow break down into an unstable pattern in which there is a churning or oscillatory motion of liquid. This flow occurs more predominantly in wide-bore tubes and may not be so important in narrow-bore tubes where the region of churn flow is small.

(d) *Annular flow*: This configuration is characterized by liquid travelling as a film on the Channel walls, and gases flowing through the center. Part of the liquid can be carried as droplets in the central gas core.

(e) *Mist flow*: The velocity of the continuous gas phase is so high that it reaches as far as the tube wall and entrains the liquid in the form of droplets.

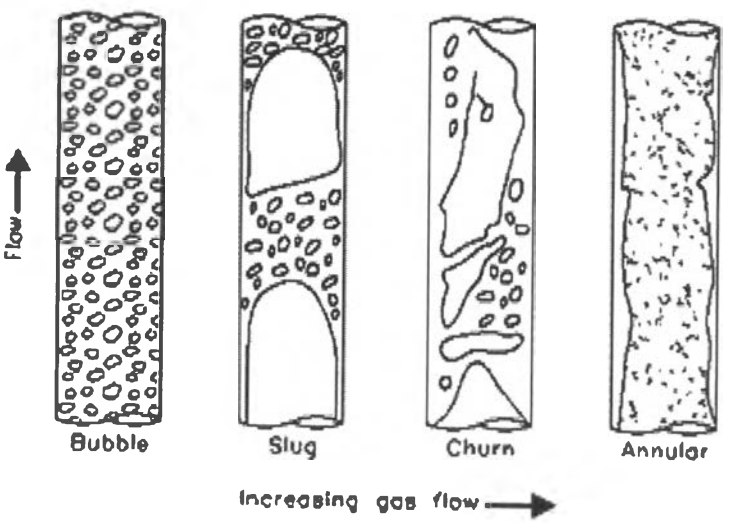

Figure 2.1 Modeling flow pattern transitions for steady Upward Gas-liquid Flow in Vertical Tubes (Bornea, and Dukler, 1980).

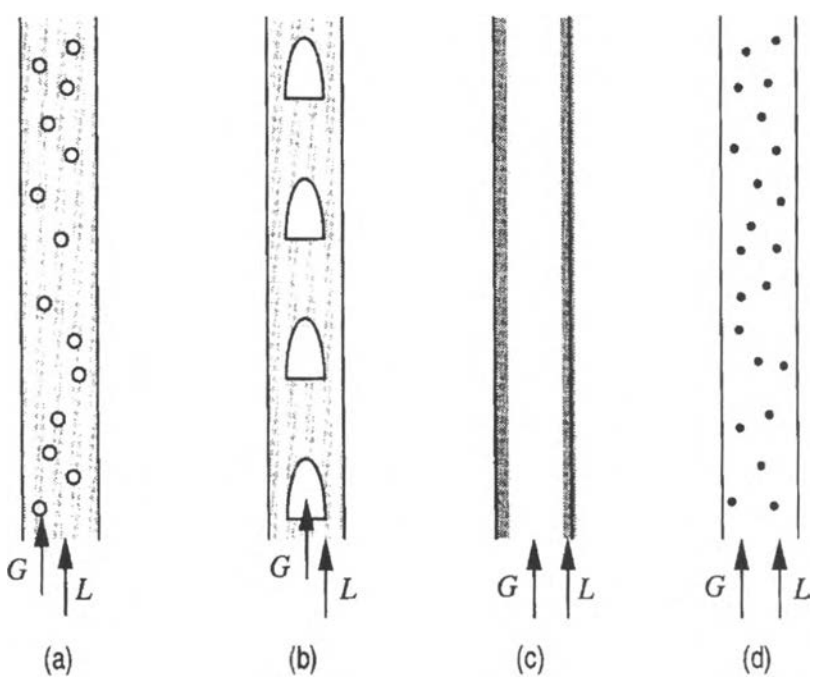

Figure 2.2 Two-phase flow regimes in a vertical tube: (a) bubble, (b) slug, (c) annular, and (d) mist flow. In each case, the gas is shown in white, and the liquid is shaded in black (Wilkes, 1999).

2.1.1.1 Bubble Flow

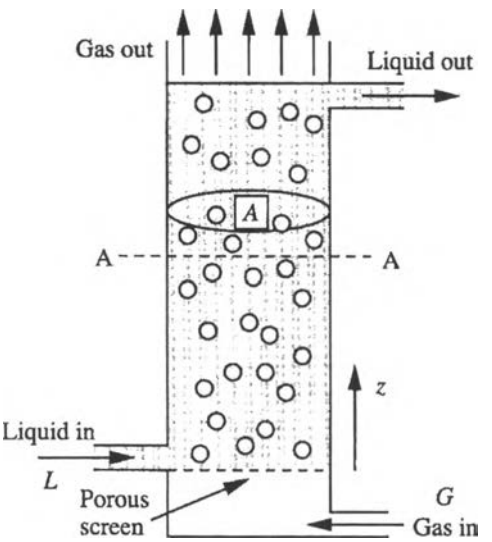

Figure 2.3 Bubble flow (Wilkes, 1999).

Gas bubbles and liquid in upward co-current flow are shown in Figure 2.3. The mean upward liquid velocity across plane A-A is

$$\bar{u}_l = \frac{G+L}{A} \qquad (1)$$

The rise velocity of gas bubbles below plane A-A is relative to a moving liquid which has a velocity ($\bar{u}_l$), so that velocity of the gas bubbles is:

$$v_g = \bar{u}_l + u_b = \frac{G+L}{A} \qquad (2)$$

where u_b is the bubble velocity rising into a stagnant liquid and total volumetric flow rate of gas is:

$$G = \varepsilon A v_g \qquad (3)$$

so the void fraction is given by:

$$\frac{G}{\varepsilon A} = \frac{G+L}{A} + u_b \quad \text{or} \quad \varepsilon = \frac{G}{G+L+u_b A} \qquad (4)$$

2.1.1.2 Slug Flow

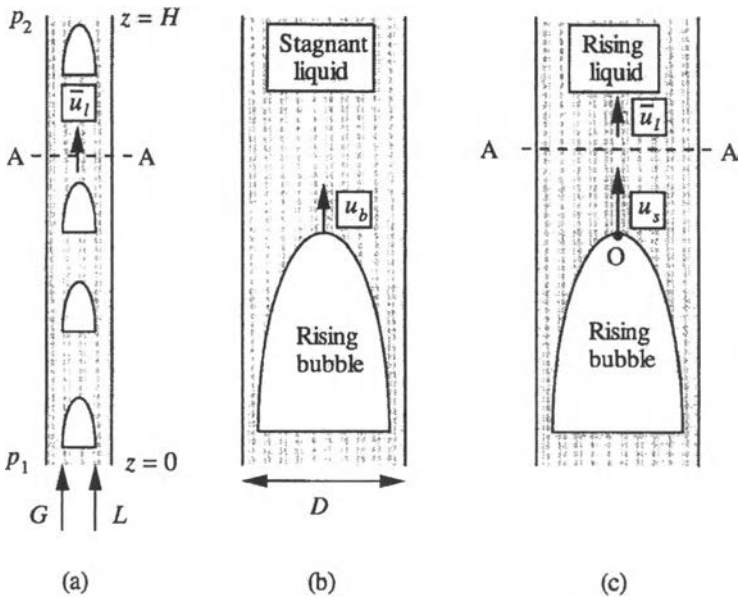

Figure 2.4 Two-phase slug flow in a vertical pipe: (a) gas and liquid ascending; (b) bubble rising in stagnant liquid; (c) bubble rising in moving liquid (Wilkes, 1999).

Figure 2.4 (a) shows the gas and liquid flow upwards together at single volumetric flow rates G and L, in a pipe of internal diameter D. An upwards liquid velocity (u_l) across a plane A-A leading of a gas slug. The total upward volumetric flow rate of liquid across A-A should be the linked gas and liquid flow rates which enter at the bottom. Therefore the mean liquid velocity at plane A-A is $\bar{u}_l=(G+L)/ A$, in which A is the cross-sectional area of the pipe.

An unlike situation of a single bubble is shown in Figure 2.4 (b). A single bubble is moving steadily upward with a rise velocity u_b in a stagnant liquid. Davies and Taylor (1950) used an approximate analytical solution for the non viscous liquid such as water and light oils, which is

$$u_b = c\sqrt{gD} \qquad (5)$$

where the constant (c) is equal to 0.33 and g is the gravitational acceleration. The experiments indicate that the constant should be equal to 0.35.

Figure 2.4 (c) shows the mean velocity of liquid and the highest velocity at the center of the pipe-near the nose of the slug. Nicklin, Wilkes, and Davision, show the value of liquid velocity of about $1.2\bar{u}_l$, and the Reynolds numbers are greater than 8,000.

Hence, the true rise velocity of the slug is:

$$u_s = 1.2\frac{G+L}{A} + u_b = 1.2\frac{G+L}{A} + 0.35\sqrt{gD} \qquad (6)$$

For the conservation of the gas; it gives:

$$G = u_s A\varepsilon \qquad (7)$$

Substituting u_s in equation (7) to (6)

$$\frac{G}{\varepsilon A} = 1.2\frac{G+L}{A} + 0.35\sqrt{gD} \qquad (8)$$

The equation (8) can be solved for the void fraction when the gas and liquid flow rates are known.

2.1.2 Air-Lift Pump Operation

A gas-lift pump uses the buoyant action of a volumetric flow rate of gas which serves to lift liquid from a height of H_0 in a reservoir to a height of H in a vertical pipe of diameter; D and cross-sectional area; A, as shown in Figure 2.5. The slug flow is assumed and liquid friction in both the supply pipe and in the vertical pipe is neglected.

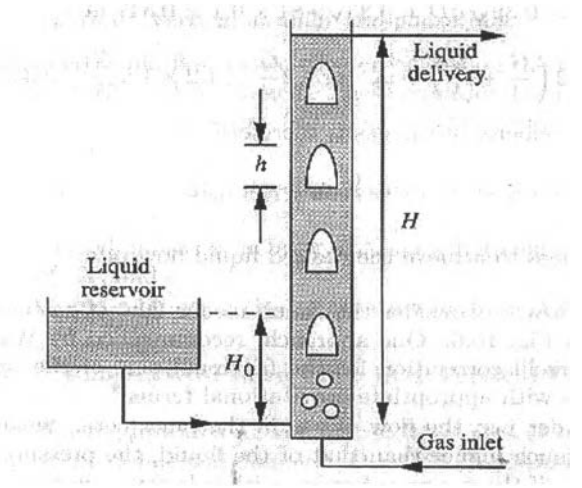

Figure 2.5 Model of gas-lift pump (Wilkes, 1999).

From hydrodynamics, the pressure at the base of the column is obtained from this below equation;

$$\rho_L g H_0 = \rho_L g H(1-\varepsilon)$$

Which gives:

$$\varepsilon = 1 - \frac{H_0}{H} \tag{9}$$

From equation (5) and (6) with L equal to 0

$$\frac{G}{\varepsilon A} = 1.2\frac{G}{A} + U_b = 1.2\frac{G}{A} + c\sqrt{gD}$$

$$\frac{G}{A}\left(\frac{1}{\varepsilon} - 1.2\right) = c\sqrt{gD}$$

$$\frac{G}{A} = \frac{c\sqrt{gD}}{\left(\frac{1}{\varepsilon} - 1.2\right)} \tag{10}$$

Substituting equation (9) into equation (10); it gives superficial velocity of gas which then suffices to achieve the desired liquid flow rate.

2.1.3 Flooding

Column containing a packing material, such as Raschig rings, is frequently used as absorbers. Packing materials inside the columns cause gas and liquid contact. A gas stream containing the component to be removed is forced up the column by a blower or compressor, while a stream of liquid flows down the tower under the influence of gravity. During this counter-current flow, the permeable component is absorbed into the liquid phase. An alternative use for a packed column is as a scrubber. In this system, the liquid phase contains the component which is scrubbed or stripped by the gas phase.

Packing

Tower packings are divided into two major types, random and regular, and should have the following characteristics:

1. High interfacial or active surface between the liquid and gas per unit volume.
2. High void space or porosity.
3. Uniform distribution of the above items 1 and 2
4. Mechanical strength to withstand normal loads in service and handling.
5. Chemical inertness.
6. Low cost.

Pressure Drop For Counter-Current Gas-Liquid Flow

When air and water flow counter-currently through a packed column, the relationship between the pressure drop and the flow rates is somewhat complicated. Figure 2.6 shows the pressure drop in a typical column as a function of superficial gas flow rate for various liquid loadings.

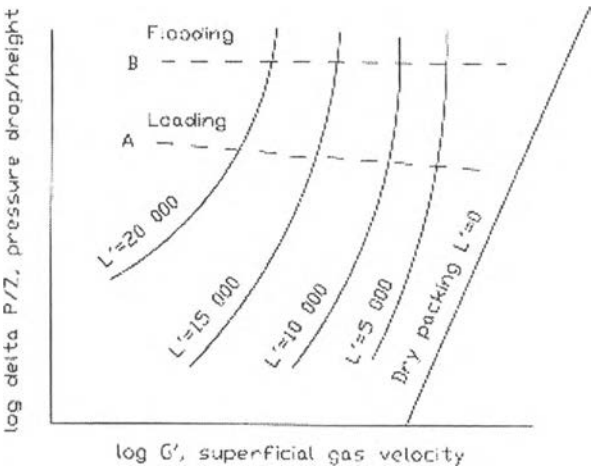

Figure 2.6 Typical gas pressure drop for counter-current flow of liquid and gas for random and structure packings (Treybal, 1980).

At a given liquid flow rate, the gas flow rate is increased until it reached at which the upwards drag exerted on the liquid by the gas appreciably counterbalances the weight of the liquid in the column and the hold-up of liquid in the column. This point is known as the ***loading point***, where the liquid no longer flows freely down the column and the hold-up of liquid in the column increases. As the gas velocity is increased further, a condition known as the ***flooding point*** is eventually reached. The approach to flooding is indicated by a rapid increasing pressure drop across the packing, liquid may fill the tower, starting at the bottom, and the column changes from gas-continuous liquid-dispersed to gas-dispersed liquid-continuous. The flooding condition can be readily observed in a transparent column. It is not practical to operate the column in a flood condition and most towers operate at below the loading point.

It is not easy to predict the curve in Figure 2.6 theoretically. In the design of a packed column it is desirable to know the gas flow rate at the flooding point since the limit of loading cannot readily be correlated. The generalized pressure drop correlation of Eckert shown in Figure 2.7 is the most widely used.

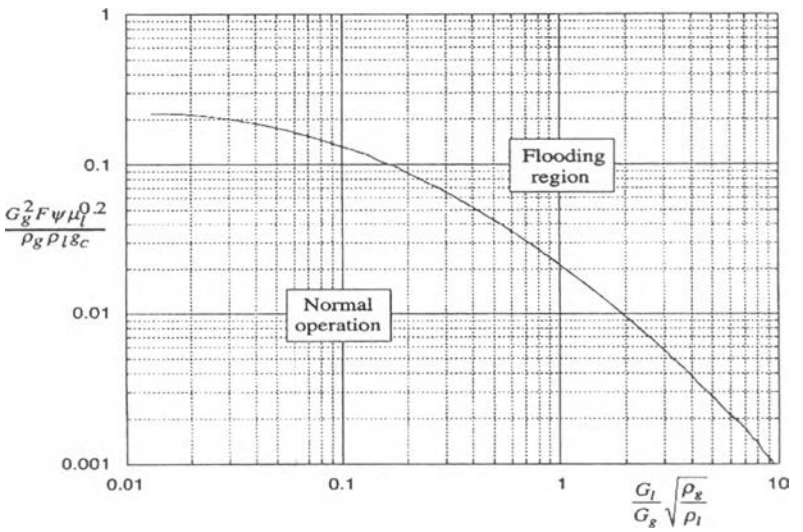

Fig. 10.9 Correlation for flooding in packed columns.

Figure 2.7 Correlation for flooding in packed columns (Eckert, 1984).

2.2 Literature Survey

2.2.1 Two-Phase Flow

Nicklin (1962) studied the properties of long bubbles in vertical tubes. It has been shown that these bubbles rise relative to the liquid ahead at a velocity exactly equal to the rising velocity of wakeless bubbles of the type studied by Dumitrescu and Taylor (1950). For 1 inch tubes, this velocity is closely predicted by motion of bubbles in moving liquid streams studied, and the results have been applied to the problem of two-phase slug flow. An expression for the voidage in steady two-phase slug flow has been derived, and this predicted voidage agrees well with the experimental results.

The study carried out by Davies and Taylor (1950) can be divided into two parts. Part I describes measurements of the shape and rising rate of air bubbles varying with the volume of 1.5 to 200 cm^3 when the rise through nitrobenzene or water. Measurements of photographs of bubbles formed in nitrobenzene show that the greater part of the upper surface is always spherical. A theoretical discussion is based on the assumption that the pressure over the front of the bubbles is the same as

that in ideal hydrodynamic flow round a sphere. The rise velocity, U, should be related to the radius of curvature, R, in the region of the vertex, by the equation $U=(2/3)\sqrt{(gR)}$; the agreement between this relationship and the experimental results is excellent. For geometrically similar bubbles of such large diameter that the drag coefficient would be independent of Reynold's number, it would be expected that U would be proportional to the sixth root of the volume, V; measurements of eighty eight bubbles show considerable scatter in the values of $U/V^{1/6}$, although there is no systematic variation in the value of this ratio with the volume.

Part II reveals that though the characteristics of a large bubble are associated with the observed fact that the hydrodynamic pressure on the front of a spherical cap moving through a fluid is nearly the same as that on a complete sphere, the mechanics of a rising bubble cannot be completely understood till the observed pressure distribution on a spherical cap is understood. Failing this can cause the case of a large bubble running up a circular tube filled with water and emptying at the bottom, which is capable of being analyzed completely, since the bubble is not then followed by a wake. An approximate calculation shows that the rise velocity U is $U=0.46\sqrt{(ga)}$, where a is the radius of the tube. Experiments with a tube with diameter of 7.9 cm gave values of U from 29.1 to 30.6 cm/sec, corresponding with values of $U/\sqrt{(ga)}$ from 0.466 to 0.490.

Choe and Hans (1996) showed that a dynamic two-phase well control model accurately analyzes the behavior of kick fluids based on a realistic assumption of unsteady state two-phase mixture flow. Two new sets of finite difference equations are developed to account for the effect of changing flow geometry. Therefore, the model is applicable for realistic two-phase well control simulation in wells with variable flow geometry. This two-phase well control model works for onshore and offshore wells with water-based mud. Pressure responses during well control operations are analyzed by the solution of conservation of mass and conservation of momentum equations. The model also includes the effect of well control method, formation influx and bubble rise velocity.

Cheng *et al.* (1997) made further investigation from bubbly flow, in an attempt to decide whether the instability of void fraction waves or a gradual

coalescence process is the cause of the bubble-to-slug transition. This was achieved by measuring the variation of bubble properties (size, velocity and density distribution) with column height and also the propagation of void fraction waves along the column as the transition was approached. Bubble properties was determined using a double resistively needle probe, and the void fraction was measured with an impedance void fraction meter (IVFM) with guarding electrodes in a 150 mm diameter column.

Experimental measurements of bubble size and void fraction wave have been completed in the 150 mm diameter column. A series of bubbles size measurements have been carried out at constant water velocity of 0, 0.64 and 1.25 m/s; with mean void fractions measured by manometer in the range of 0.06 - 0.41 and marginally higher station. The measurements of void fraction waves in the 150 mm diameter column are performed at three constant water velocities of 0, 0.32 and 0.65 m/s, with mean void fraction in the range of 0.05 - 0.52, and at two constant gas velocities of 0.426 and 0.737 m/s, with mean void fractions covering a similar range. In the 28.9 mm diameter column, void fraction wave measurements have been carried out at one constant water velocity of 0.65 m/s only, with the bubble generator run to produce a small bubble size (although the size has not yet been measured) and the mean void fraction varied from 0.073 to 0.3373 at the bottom and from 0.09995 to 0.4273 at the top.

The results show that traditional slug flow does not exist in 150 mm diameter column. Instead, there is a very gradual transition to a type of churn flow as gas rate is increased. Bubble size, both mean and median chord lengths, decreases with height and the bubble frequency increases. This suggests bubble break-up rather than coalesce, although there is some evidence of an increase in the maximum size of cap bubbles found at high gas rates. When increasing gas rate at constant liquid rate in the 150 mm column, the gain factor gradually increases through 1.0, and the SNR passes through a maximum at the visually observed onset of large flow structures. There is no such obvious trend when the liquid rate is reduced at constant gas rate, and although the same transition is observed visually, the system gain factor remains above 1.0: gain factor alone is clearly not a suitable criterion for judging the transition. In the 28.9 mm column, increasing the gas rate at constant liquid rate

leads to a sudden transition to slug flow, with a jump in the gain factor greater than 1.0, and also in the SNR. The suddenness of the transition suggests an instability mechanism, rather than a gradual coalescence. The cause of the gradual transition in the 150 mm column remains unclear.

Ohnuki and Akimoto (1999) showed that in order to investigate the dependency of gas-liquid flow on pipe scale, the transition characteristics of flow pattern and phase distribution were studied experimentally in upward in air-water flow along a large vertical pipe (D: 0.2 m, L/D: 61.5). The experiments were conducted under the flow rate: 0.03 m/s $\leq J_G \leq$ 4.7 m/s (at top of test section), 0.06 m/s $\leq J_L \leq$ 1.06 m/s. Flow pattern was observed and measurements were performed on axial differential pressure, phase distribution, bubble size and bubble and water velocities. The scale effect on the phase distribution was discussed with small-scale data by Leung *et al.* (1995) and Liu and Bankoff (1993 a, b).

As for the flow pattern, the flow conditions at which coalescence starts are almost the same as those found in small-scale pipes, but no large bubbles are observed in the region L/D lower than 20 which corresponds to the developing region of the axial differential pressure curves. The large coalescent bubbles were generated in L/D greater than 20. The churn flow is dominant in the large vertical pipe under the conditions where small-scale pipes have slug flow. In contrast to small-scale pipes, the agitation of flow pattern is likely to be occurred under a lower J_L in the bubbly flow and under the flow pattern with large coalescent bubbles. Under the agitated bubbly flow, some large eddies including bubble clusters fill up the pipe. The flow direction of a cluster is frequently observed. In the churn slug/froth flow region, large coalescent bobbles flow in the liquid film region between the large bubble and the wall.

The transition of phase distribution corresponds to the change of flow pattern. Large coalescent bubbles affect the phase distribution as similar to small-scale pipes but the core-peak phase distribution is established in the agitated bubbly flow under a low J_L where small-scale pipes have a wall-peak phase distribution. The large coalescent bubbles are developed along the test section via the churn bubbly flow where the phase distribution is a core peak one, whereas Taylor bubbles

in small-scale pipes are generated at the vicinity of gas-liquid mixing region or are developed from the bubbly flow with a wall-peak phase distribution. The wall-peak in the large vertical pipe is lower even under the same bubble size. The lower peak is considered to be related to the lower radial velocity gradient of water and the larger turbulent dispersion force. More quantitative studies are needed for the scale effect on the contribution of liquid turbulent kinetic energy and on the threshold value of bubble size giving the transition from the wall-peak to the core-peak phase distribution. Detailed measurements are also needed to investigate the flow structure under the agitated bubbly flow.

2.2.2 Flooding

A method for the estimation of gas velocity at the flooding point of various packings, is based on such fundamental parameters as the porosity and specific surface of the packing itself. Methods for estimating the flood conditions have been studied and developed for several decades.

Sherwood *et al.* (1938) who originally proposed the form of the GDPC chart (Generalized Pressure Drop Correlation). Although not perfect, the original GDPC provides a satisfactory estimation of the unit pressure drop ($\Delta p/H$) through irrigated packing. Nevertheless, among other parameters characteristic of the packing, knowledge of both the porosity and specific surface area is still essential. The Sherwood-type correlation chart has been adapted by others, and thus, several modified versions of the original GDPC are accessible today.

Eckert *et al.* (1966, 1970, 1975) showed that some of these versions differ from the initial one by the ordinate only. Substitution of the a/ε^3 by the factor F_p, is a key modification in the correlations concerned. F_p, an empirical value, which is characteristic of each packing and moreover, depends on the hydrodynamic conditions in the tower is called the packing factor. Therefore, for the same packing element, varied values of the packing factor are available in the open literature. Futhermore, preliminary analyses clearly proved a large scatter of empirical values of the factor F_p, against those calculated according to Eckert's version and on the

assumption that F_p equal to a/ε^3. It is also worth nothing the inconsistencies in the interpretation of this factory by different authors.

Due to all the aforementioned limitations, originated from the GDPC chart, estimation of gas velocity at the flooding point is a rather hard task; since, in any case, despite the original version of that chart, it is also necessary to know the empirical constants specific for a given packing.

Taking the Ergun model as a basis, Kaiser (1994) proposed an estimation of the flooding-point gas velocity as that beginning derived directly from the curve plotted on the strength of the empirically founded factor, K_0. On the other hand, Lockett (1995) suggested a flood curve based on the equations determined with the countercurrent flow of liquid and vapor phases (two-phase countercurrent flow model) through the pipe. In these equations, A_c and m are empirical constants provided by Lockett, for Mellapak Y only. In his work, Kister (1992) indicates the Billet and Schultes correlation model equations as those useful for estimation of gas velocities at the flooding point. To apply this system of model equations, however, it is necessary to know either C_1 or C_2 empirical constants. The same refers to equations conceived by Mackowiak (1991 a, b), using the droplet-suspended-bed model. Applying correlations based on this model is only possible, if the drag coefficient, Ψ_{fl}, for the single-phase flow is known.

To estimate the phase velocities at the flooding point for the air/water system, Kuzniewska-Lach (1996) proposed a method is about ±10 %, in comparison with the droplet-suspended-bed model (Mackowiak, 1991 a), and by comparison with the Sherwood et al. (1938) correlation chart, the error oscillates between ±20 %.